

Spatially Resolved Electron Density Measurements Using the Balmer H_{β} Line

GHANESHWAR GAUTAM AND CHRISTIAN G. PARIGGER

*The University of Tennessee / UT Space Institute,
Center for Laser Applications,
411 B.H. Goethert Parkway,
Tullahoma, TN 37388-9700, USA*

ABSTRACT: In this work, Balmer series hydrogen beta electron density diagnostics in laser-induced plasma are of interest. A pressure cell was filled with pure hydrogen gas at 810 ± 25 Torr, and micro-plasma is generated by using Nd:YAG laser radiation at the wavelength of 1064 nm. Temporally and spatially resolved spectra were collected with the use of spectrometer-detector system. Electron densities of the micro-plasma from FWHM and peak separation of the Stark broadened hydrogen Balmer H_{β} line are determined and compared at 400 ns and 650 ns time delays. Spatial variation of the electron density is also investigated for these time delays. The measured peak separation values from the data, smoothed by using Savitzky-Golay filter, indicate smaller values for the electron densities than determined from FWHM. However, fitting the measured Stark broadened line profile data with the computer simulated profile shows consistent results for an electron density of the order of $1 \times 10^{17} \text{ cm}^{-3}$.

PACS codes: 52.38.Mf, 32.70.Jz, 33.70.Jg

KEYWORDS: Atomic Spectroscopy, Stark broadening, Plasma diagnostics, Peak separation, Electron density

1. INTRODUCTION:

Stark broadened spectral profiles of the hydrogen Balmer beta line, H_{β} , are used to determine the plasma electron density, N_e . The full width at half maxima (FWHM) and wavelength separation between the peaks of the H_{β} line are used to determine the electron density. The H_{β} line is one of the most studied line shape in plasma emission spectroscopy and can be utilized for electron number density up to $7 \times 10^{17} \text{ cm}^{-3}$. In 1919, Holtsmark derived the distribution applicable to plasma physics [1]. Holtsmark distributions are utilized to evaluate Stark broadened profiles of H_{β} [2]. The results for Stark broadened H_{β} are consistent with the generalized theory of Stark broadening [3]. However, the technique can only be applied for optically thin line profiles.

The use of peak-separation values for finding N_e is elaborated with respect to its application as a plasma electron density diagnostic. Spatial variation of the electron density is determined by utilizing both the FWHM and peak separation methods. When fitting with the computer simulated profile [4, 5], the peak separation method shows consistent result with the result from FWHM for electron densities of the order of $1 \times 10^{17} \text{ cm}^{-3}$.

2. EXPERIMENTAL DETAILS

Temporally and spatially resolved atomic spectra from the micro-plasma are collected for the purpose of evaluating the electron density and its spatial variation. For micro-plasma generation in pure hydrogen gas, a pressure cell was evacuated with the help of a diffusion pump and filled with a hydrogen gas at a pressure of 810 ± 25 Torr. The

data were recorded with a 20 ns gate width. An average of 50 consecutive laser-plasma events was accumulated. The recorded spectra are wavelength calibrated and detector-sensitivity corrected. The electron density evaluations from the Stark width and the H_{β} peak separation are performed by using the formulae for peak separation and full-width-half-maximum (FWHM), see Equations (1) and (2) in the experimental results section. In the conditions of our experiment, Doppler and instrumental broadenings are negligible in comparison to the Stark broadening.

The experimental arrangement consists of a Q-switched; Nd:YAG laser with a frequency of 10 Hz generating 13 ns pulses with an energy of 190 mJ, operated at the fundamental wavelength of 1064 nm. Synchronization of the various instruments used is achieved for the time-resolved measurements. The laser travel time from the exit aperture of the Nd:YAG laser to the spectrometer slit is accounted for the data measurements. Figure 1 illustrates the experimental arrangement.

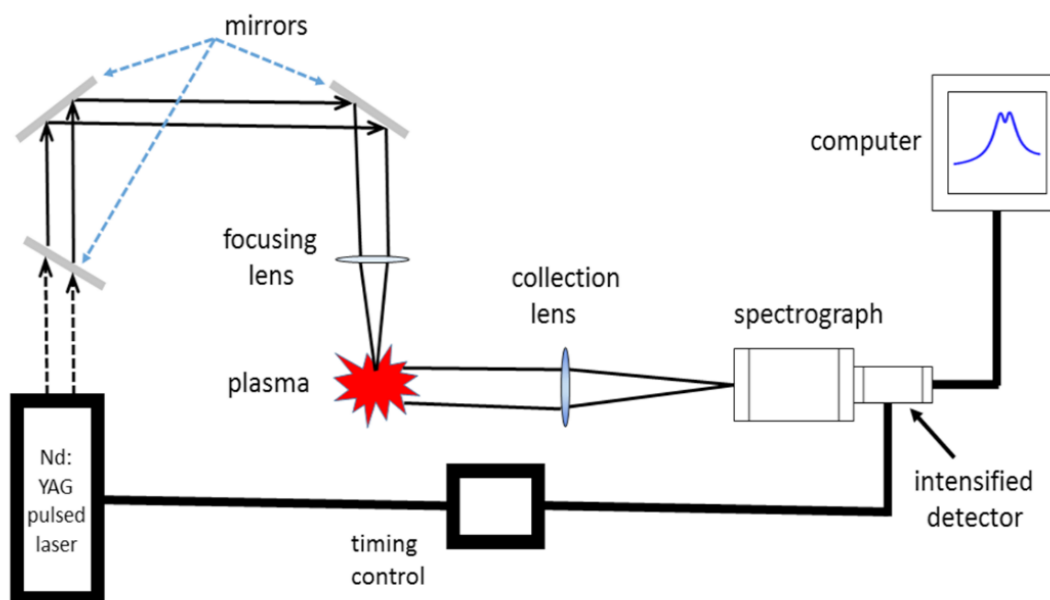


Figure 1: Experimental schematic for LIBS with the Nd:YAG laser source, mirror, focusing and collection lens for the micro-plasma radiation.

Three mirrors and a lens are used to direct and focus the beam as shown in the above diagram. The generated micro-plasma is imaged onto the spectrometer slit by two uncoated, fused silica lenses. In the experiments discussed here, a 1200 grooves/mm grating is selected to disperse the radiation from the plasma for various time-resolved spectroscopic studies with a 0.64 m Jobin-Yvon spectrometer and a spectrometer-detector system of resolution 0.10 nm. A 2-dimensional charge coupled device (ICCD; Andor technology model iStar) is used to record spatially and temporally resolved images along the slit height. Further details about the experimental arrangement are given in Ref. [6].

3. EXPERIMENTAL RESULTS

Figure 2 displays the recorded plasma spectra of H_{β} generated in pure hydrogen gas (99.999 purity) at 400 ns and 650 ns time delays. The displayed data are wavelength calibrated and intensity corrected. The intensity calibration was accomplished with deuterium/tungsten (Ocean Optics model DH-2000) calibration lamp.

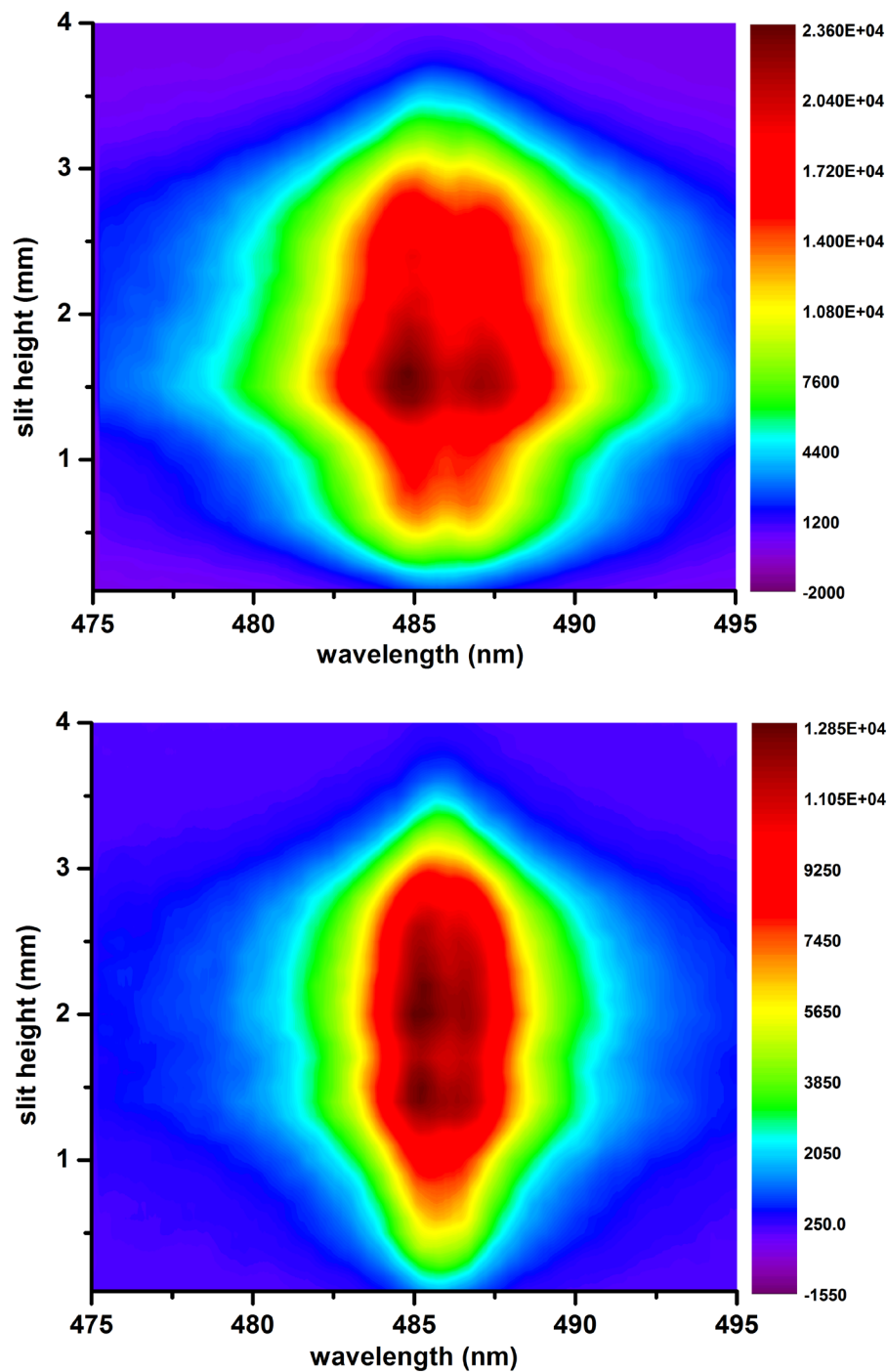


Figure 2: Experimental plasma spectra of hydrogen Balmer beta line in pure hydrogen gas at 400 ns (top) and 650 ns (bottom) time delays.

To record these spectra, laser radiation was focused from the top of the image, therefore, we would expect slightly lower electron densities towards the bottom of the image. A program in Matlab was used for the data management and calibration, furthermore, Origin 8.1 software was employed to generate contour plots.

The electron density is determined from the hydrogen beta line [5, 10], reproduced here:

$$N_{e,\beta} [m^{-3}] = \left[\frac{\Delta\lambda [\text{nm}]}{4.8} \right]^{1.46808} \times 10^{23} \quad (1)$$

$$\log N_{e,\beta} [m^{-3}] = 22.661 + 1.416 \log \Delta\lambda_{ps} [\text{nm}] \quad (2)$$

The empirical electron density formula in Eq. (1) and (2) shows a close to 3/2 power dependence of the FWHM and peak separation values. Therefore, the error margins for the electron densities are 1.5 times the error margins of the FWHM and peak separation. The electron density results from FWHM and peak-separation should be in agreement within the error margin of H_{β} [11] for N_e of the order of $1 \times 10^{17} \text{ cm}^{-3}$. Disagreements may arise due to difficulties in extracting the peak wavelengths from individual data lines to determine the peak separation values. The application of Eq. (2) also inherently introduces additional (minor) errors due to absence of electron temperature T_e and reduced mass μ [10, 11, 12]. Small amount of background continuum may further introduce some error in these values.

Tables 1 and 2 show the results of our analysis of the central range of 16 of the 50 line spectra that were recorded. In this central range, the H_{β} peak-separations could be extracted to find the electron densities along the plasma. Each of the line spectra is recorded by using pinning of 8 vertical pixels corresponding to approximately 0.11 mm in the 1.05:1 imaging of the plasma. The FWHM and peak-separation of the Stark broadened H_{β} lines are used to find the indicated values of the electron density variations of the plasma. The results in the tables display the overall trend of a decreasing electron density from top to bottom with some exceptions. The data for the peak separation method are smoothed by using 51 point Savitzky-Golay filter yet errors persist in finding the peak separation. The Matlab program was used to extract values of peak separation. The directly measured peak separation indicates smaller N_e values than expected from FWHM. When fitting the measured with computer simulated profiles for an electron densities of the order of $1 \times 10^{17} \text{ cm}^{-3}$, the peak separation and FWHM will yield consistent results [7]. Results in Tables 1 and 2 are also in agreement with the previous experiment done in pure hydrogen gas using similar type of experimental conditions [8, 9].

Table 1

Spatial variation of electron densities at different time delays for pure hydrogen gas from FWHM of Stark broadened line profiles (slit height 2.9 to 1.2 mm, top to bottom).

<i>FWHM (nm) at 400 ns</i>	<i>Electron density (cm^{-3}) $\times 10^{17}$</i>	<i>FWHM (nm) at 650 ns</i>	<i>Electron density (cm^{-3}) $\times 10^{17}$</i>
9.44	2.70	5.35	1.17
9.34	2.66	5.30	1.16
9.48	2.72	5.32	1.16
9.41	2.69	5.30	1.16
9.13	2.57	5.30	1.16
9.25	2.62	5.41	1.19
9.13	2.57	5.60	1.25
9.11	2.56	5.62	1.26
9.11	2.56	5.51	1.22

8.97	2.50	5.41	1.19
8.88	2.47	5.30	1.16
8.51	2.32	5.25	1.14
8.71	2.40	5.11	1.10
8.46	2.30	5.04	1.08
8.32	2.24	4.76	0.99
6.88	1.70	4.49	0.91

Table 2
Spatial variation of electron density at different time delays for pure hydrogen gas from peak-separation of Stark broadened line profiles (slit height 2.9 to 1.2 mm, top to bottom).

<i>Peak-separation (nm) at 400 ns</i>	<i>Electron density (cm⁻³) × 10¹⁷</i>	<i>Peak-separation (nm) at 650 ns</i>	<i>Electron density (cm⁻³) × 10¹⁷</i>
2.60	1.78	1.37	0.72
2.56	1.73	1.32	0.68
2.53	1.71	1.46	0.79
2.53	1.71	1.49	0.80
2.46	1.64	1.32	0.68
2.30	1.49	1.46	0.79
2.30	1.49	1.44	0.77
2.14	1.34	1.30	0.67
2.09	1.30	1.30	0.67
2.23	1.43	1.20	0.60
2.37	1.56	1.49	0.80
2.25	1.45	1.32	0.68
2.42	1.60	1.25	0.63
2.05	1.26	1.02	0.47
2.39	1.58	1.28	0.65
1.84	1.09	1.09	0.52

Figures 3 and 4 display measured data points and the fitted computer-simulated profiles using symmetric hydrogen beta lines at 400 ns and 650 ns time delays. Yet, the Balmer beta lines show asymmetric profiles due to ion dynamics [13] in the investigated range of electron densities. This asymmetry can be seen in the experimental data points. Fitted profiles are obtained by using computer simulations [4, 5] which includes ion dynamics effects as well, yet we used symmetric profiles for this analysis. Measured values of the peak separation from these fitted profiles yields consistent results for electron densities of the order of $1 \times 10^{17} \text{ cm}^{-3}$. Previously, we also used the Origin software to fit double-peak Lorentzians and/or Voigt profiles to recorded hydrogen beta lines; however, such fitting would show a decrease in the peak separation due to the two Lorentzians. Fitting the measured line profile with the computer simulated hydrogen beta line is preferred to determine the electron density.

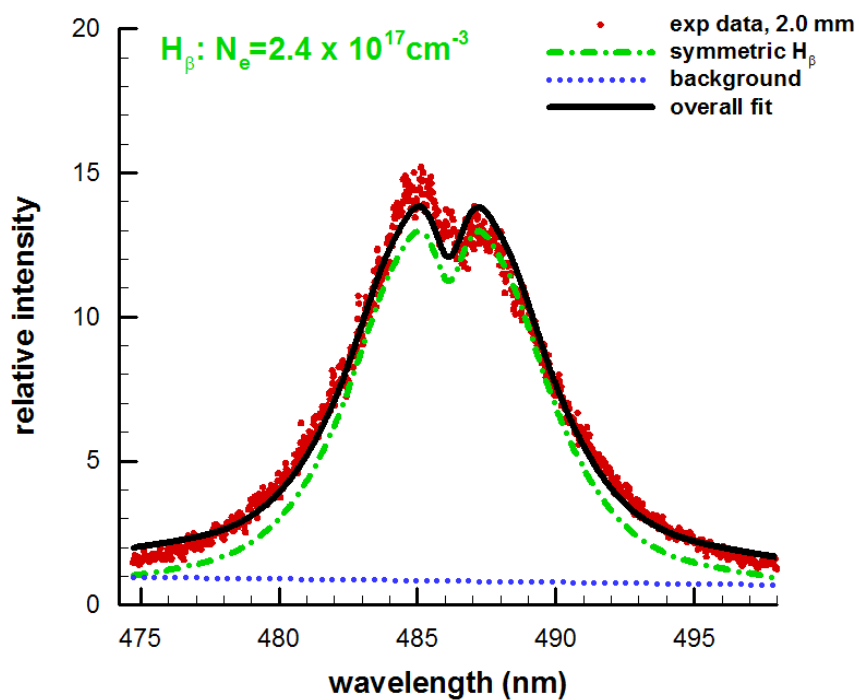


Figure 3: Measured and fitted H_{β} profiles, 400 ns time delay, slight height 2 mm.

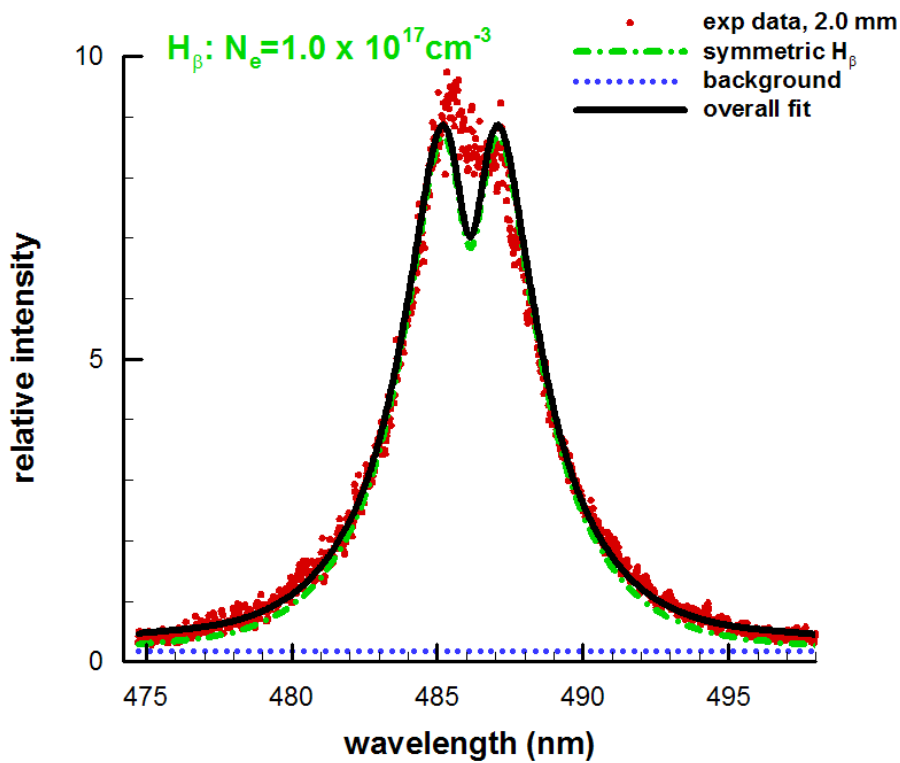


Figure 4: Measured and fitted H_{β} profiles, 650 ns time delay, slight height 2 mm.

4. CONCLUSIONS

Electron densities are determined from the hydrogen Balmer series, H_β, line widths and peak-separations. The peak-separation method compared with the well-established FWHM method shows reliable results when (i) the values of the peak separations are extracted from the computer simulated profile fitted with the experimental data points, and (ii) when the electron density is of the order of $1 \times 10^{17} \text{ cm}^{-3}$. However, directly extracted peak separation values from the noisy data indicate lower electron densities than obtained from FWHM values. In the central region of the micro-plasma, the determined electron densities for the 400 ns and 650 ns time delays reveal slightly higher values towards the upper portion of the micro-plasma. For time delays of 150 ns after plasma generation, the measurements show incomplete profiles in the 474 nm to 498 nm window, indicating electron densities of the order of $7.5 \times 10^{17} \text{ cm}^{-3}$. Analysis of the recorded data in pure hydrogen for such time delays is of continued interest.

Acknowledgments

The authors greatly appreciate support in part for this work by the Center for Laser Applications at The University of Tennessee Space Institute.

References

- [1] J. P. Holtzmark, *Ann. Phy.* 338 (1919) 577-630.
- [2] H. R. Griem, *Plasma Spectroscopy*, McGraw-Hill, (1964).
- [3] E. Oks, *Stark Broadening of Hydrogen and Hydrogenlike Spectral Lines in Plasmas, The Physical Insight*, Alpha Science(2006).
- [4] M.A. Gigosos, V. Cardeñoso, *J. Phys. B : At. Mol. Opt. Phys.* 29 (1996) 4795-4838.
- [5] M.A. Gigosos, M.Á. González, V. Cardeñoso, *Spectrochim. Acta B* 58 (2003) 1489-1504.
- [6] C.G. Parigger, A.C. Woods, M.J. Witte, L.D. Swafford, D.M. Surmick, *J. Vis. Exp.* 84 (2014) E51250.
- [7] G. Gautam, C.G. Parigger, D.M. Surmick, A. M. El. Sherbini, Laser plasma diagnostics and self-absorption measurements of the H_β Balmer series line, *J. Quant. Spect. Radiat. Transf.* 170 (2016) 189-193.
- [8] C. G. Parigger, *Spectrochim. Acta B* 79-80 (2013) 4-16.
- [9] C.G. Parigger, D.H. Plemmons, E.Oks, *Appl. Opt.* 42 (2003) 5992-6000.
- [10] M. Ivković, N. Konjević, Z. Pavlović, *J. Quant. Spect. Radiat. Transf.* 154 (2015) 1-8.
- [11] G. Gautam, D. M. Surmick, C. G. Parigger, *J. Quant. Spect. Radiat. Transf.* 160 (2015) 19-21.
- [12] A. M. El Sherbini, D. M. Surmick, G. Gautam, C. G. Parigger, *Int. Rev. At. Mol. Phys.* 5 (2014) 23-31.
- [13] S. Djurović, M. Cirisan, A.V. Demura, G.V. Demchenko, D. Nikolić, M.A. Gigosos, M.A. González, *Phys. Rev. E* 79 (2009) 046402.

